ACS Energy Letters

http://pubs.acs.org/journal/aelccp

LETTER

Electrified Cement Production via Anion-Mediated Electrochemical Calcium Extraction

Rui Kai Miao,[#] Ning Wang,[#] Sung-Fu Hung, Wen-Yang Huang, Jinqiang Zhang, Yong Zhao, Pengfei Ou, Sasa Wang, Jonathan P. Edwards, Cong Tian, Jingrui Han, Yi Xu, Mengyang Fan, Jianan Erick Huang, Yurou Celine Xiao, Alexander H. Ip, Hongyan Liang, Edward H. Sargent,* and David Sinton*

Cite This: *ACS Energy Lett.* 2023, 8, 4694−4701

Read Online

ABSTRACT: Cement production is a carbon-intensive industrial process, with the sector contributing ∼8% of global anthropogenic CO_2 emissions. On average, producing each kilogram of cement leads to the emission of 1 kg of CO_2—the combination of fuel combustion emissions and carbon released from the feedstock, limestone ($CaCO_3$). Here we report electrochemical cement production based on anion-mediated electrochemical calcium extraction (ECE) that addresses both feedstock and energy emissions. The *in situ*-generated acidic electrolytes release the feedstock CO_2 emissions at high purity, enabling direct carbon utilization or sequestration without costly capture and purification steps. Energy embodied within a separate H_2 output stream is sufficient to sinter $Ca(OH)_2$ to produce portland cement, thus removing the CO_2 emissions associated with fuel combustion. We then replace $CaCO_3$ with a carbon-free calcium feedstock, gypsum, thereby removing the CO_2 emissions embodied in the feedstock. Technoeconomic analysis forecasts that this method could provide a viable, decarbonized cement alternative.

Cement is a precursor to concrete—second only to water as the most used material in the world.[1−3] The global production of cement currently exceeds 4 billion metric tons annually[4] and is expected to grow 25−50% by 2050.[5,6]

Cement manufacture consumes 3% of global energy[6,7] and accounts for ∼8% of anthropogenic CO_2 emissions.[3,7,8] This share of emissions is expected to grow in the decades ahead, with persistent demand. On average, 1 kg of CO_2 is emitted for each kilogram of cement produced.[6] The production of cement clinker requires the calcination of limestone ($CaCO_3$) at ∼900 °C and subsequent sintering with SiO_2 at ∼1500 °C, and both processes are carbon intensive. The calcination process decomposes limestone into CaO and releases CO_2 (Figure 1a). These emissions are inherent to the carbon-containing feedstock and account for ∼50% of the total CO_2 emissions during cement manufacture, with fuel combustion accounting for the balance.[9,10] Although chemical and steel production present a range of opportunities for electrification and decarbonization,[11] low-carbon cement production remains a challenge.

Applying established carbon capture and purification to cement production is prohibitively costly.[12,13] Today's process emits 15−30% CO_2 in a mixture of NO_x, SO_x, and O_2 that is challenging to separate. Removing CO_2 from this post-combustion stream requires ∼4 GJ/tonne CO_2 and adds $90/tonne cement to the cost of manufacturing—a severe 2-fold increase in the current cost of cement production.[14,15]

Electrified kilns[16] and biofuel adoption[17] can reduce energy emissions but cannot address feedstock emissions—the 50% of emissions embodied within limestone. Alternative materials have been developed to replace clinker, either in part or in full, to reduce feedstock emissions.[18−22] However, these alternatives are projected to meet <5% of future demand due to barriers of availability, price, and technical limitations.[3,18,23] Achieving substantial reductions in CO_2 emissions will require addressing both the energy emissions and the carbon content embodied within the feedstock.

Synthesizing cement electrochemically provides a means to reduce energy and feedstock emissions by taking advantage of pH gradients developed in an electrolyzer.[24−26] At the locally acidic anode, $CaCO_3$ is neutralized into Ca^{2+} and CO_2. The Ca^{2+} ions migrate across the cell and combine with OH^- generated by the cathodic hydrogen evolution reaction to form $Ca(OH)_2$.

Received: August 12, 2023
Accepted: October 12, 2023
Published: October 16, 2023

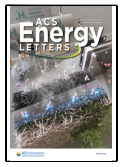

https://doi.org/10.1021/acsenergylett.3c01668
ACS Energy Lett. 2023, 8, 4694−4701

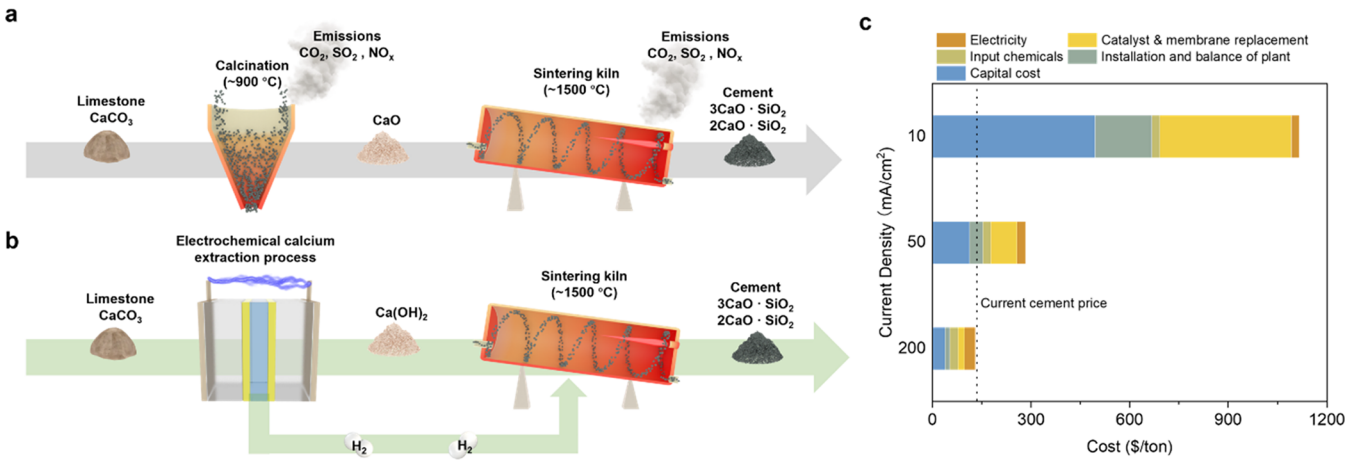

Figure 1. Electrified cement production process using electrochemical calcium extraction. Schematics illustrate (a) a conventional carbon-intensive cement production process and (b) an electrified cement production process using electrochemical calcium extraction. (c) Breakdown of electrified cement costs at different current densities.

The produced $Ca(OH)_2$ precipitate and H_2 gas can be used in the subsequent sintering process as cement feedstock and fuel, respectively. This approach has been demonstrated in a batch reactor at 10 mA/cm^2, with the potential to significantly reduce emissions.[24] However, this reaction must proceed at an industrially relevant current density (>100 mA/cm^2, Figure 1c and Note S1) to offer commercial viability. In addition, oxygen is evolved at the anode along with CO_2 in this process. Separating such a mixture adds an energy cost of ∼2 GJ/tonne cement on top of the energy requirement for the electrochemical process, doubling the energy requirement of conventional cement production (Note S2 part 1, Figure S1).

Here, we took the view that both energy and feedstock emissions could be addressed in an anion-mediated electrochemical calcium extraction (ECE) process (Figure 1b). In such a scheme, the *in situ*-generated acidic electrolytes (instead of a pH gradient) react with the limestone in a separate chamber to extract calcium cations, ensuring that the CO_2 within limestone is liberated at high purity. This high purity enables direct downstream utilization or storage without costly carbon capture and purification steps.[27,28] Incorporating highly active catalysts in a membrane-based electrolyzer, we achieve a current efficiency of 93% and a full-cell voltage of 2.8 V at 200 mA/cm^2, corresponding to an energy cost of 6.7 GJ/tonne cement—comparable with conventional cement production without CO_2 capture (Note S2 part 2, Figure S1). The cement is produced in the standard form, portland cement, compatible with the current market and regulations of the building industry. We then adapt this process to accommodate a carbon-free feedstock, gypsum ($CaSO_4{\cdot}2H_2O$), that fully eliminates feedstock emissions.

In the ECE process, limestone is first neutralized by HCl/HOCl to form high-purity gaseous CO_2 (Figure S2) and $CaCl_2$/$Ca(OCl)_2$ (eq 1, Figure 2a), a soluble salt that has sufficient conductivity to support the electrochemical reaction. The $CaCl_2$/$Ca(OCl)_2$ solution is then pumped into the anode of an electrochemical unit, where chlorine evolution takes place (eq 2a). The chlorine evolution reaction was chosen as the anodic reaction because it operates with fast kinetics[29] and regenerates the electrolyte back into a strong acid (eq 2b) for subsequent $CaCO_3$ neutralization. At the cathode, the hydrogen evolution reaction (HER) produces gaseous H_2 and hydroxide ions (eq 3). The anode and cathode are positioned on each side of a cation-exchange membrane (CEM) and an anion-exchange membrane (AEM), respectively, to deliver Ca^{2+} and OH^- ions and avoid the electrodeposition of Ca^{2+} cations on the cathode. In the gap between the membranes, Ca^{2+} (from the anode) and OH^- (from the cathode) combine into $Ca(OH)_2$ (eq 4, Figure S3). Continuous flow of a conductive NaCl electrolyte stream decreases ionic transfer losses and carries out the $Ca(OH)_2$ precipitated therein. This process has similarities to the chloralklali process, with the anion mediation here being the key differentiator and one that enables chloride recycling and formation of high-purity CO_2. The chloralkali process generates chlorine gas as the product. The chlorine gas can be used to generate concentrated hydrochloric acid for calcium neutralization. However, this process requires an additional step with heat input and demands costly corrosion-resistant materials to retain the hydrochloric acid.

$$\mathrm{HCl} + \mathrm{HOCl} + \mathrm{CaCO_3} \rightarrow \frac{1}{2}\mathrm{CaCl_2} + \frac{1}{2}\mathrm{Ca(OCl)_2} + \mathrm{CO_2} + \mathrm{H_2O} \quad (1)$$

$$2\mathrm{Cl^-} \rightarrow \mathrm{Cl_2} + 2\mathrm{e^-} \quad (2a)$$

$$\mathrm{Cl_2} + \mathrm{H_2O} \leftrightarrow \mathrm{HOCl} + \mathrm{HCl} \quad (2b)$$

$$2\mathrm{H_2O} + 2\mathrm{e^-} \rightarrow \mathrm{H_2} + 2\mathrm{OH^-} \quad (3)$$

$$\mathrm{Ca^{2+}} + 2\mathrm{OH^-} \rightarrow \mathrm{Ca(OH)_2} \quad (4)$$

To achieve efficient conversion, we used electrocatalysts with high activity and selectivity for HER and chlorine evolution reaction: platinum on carbon[30] (Pt/C, Figure S4) and iridium oxide[31] (IrO_2, Figure S5), respectively. We first operated the system at a current density of 100 mA/cm^2 to verify its effectiveness. The system voltage was ∼2.5 V, and the system operated steadily over an initial 1-h period (Figure S6a). We determined the current efficiency of the system to be 93% (Figure S7, method details in Note S3). Further increasing the current density, the applied voltages showed a linear trend, indicating that series resistance dominates the process (Figure 2b; see electrochemical impedance spectroscopy measurements and method details in Figure S9). Further extending the process by using other halides as the anion mediators (e.g., bromide and iodide) offers a reduction in the operating voltage, as these anions oxidize at lower thermodynamic potentials. Among all

https://doi.org/10.1021/acsenergylett.3c01668
ACS Energy Lett. 2023, 8, 4694−4701

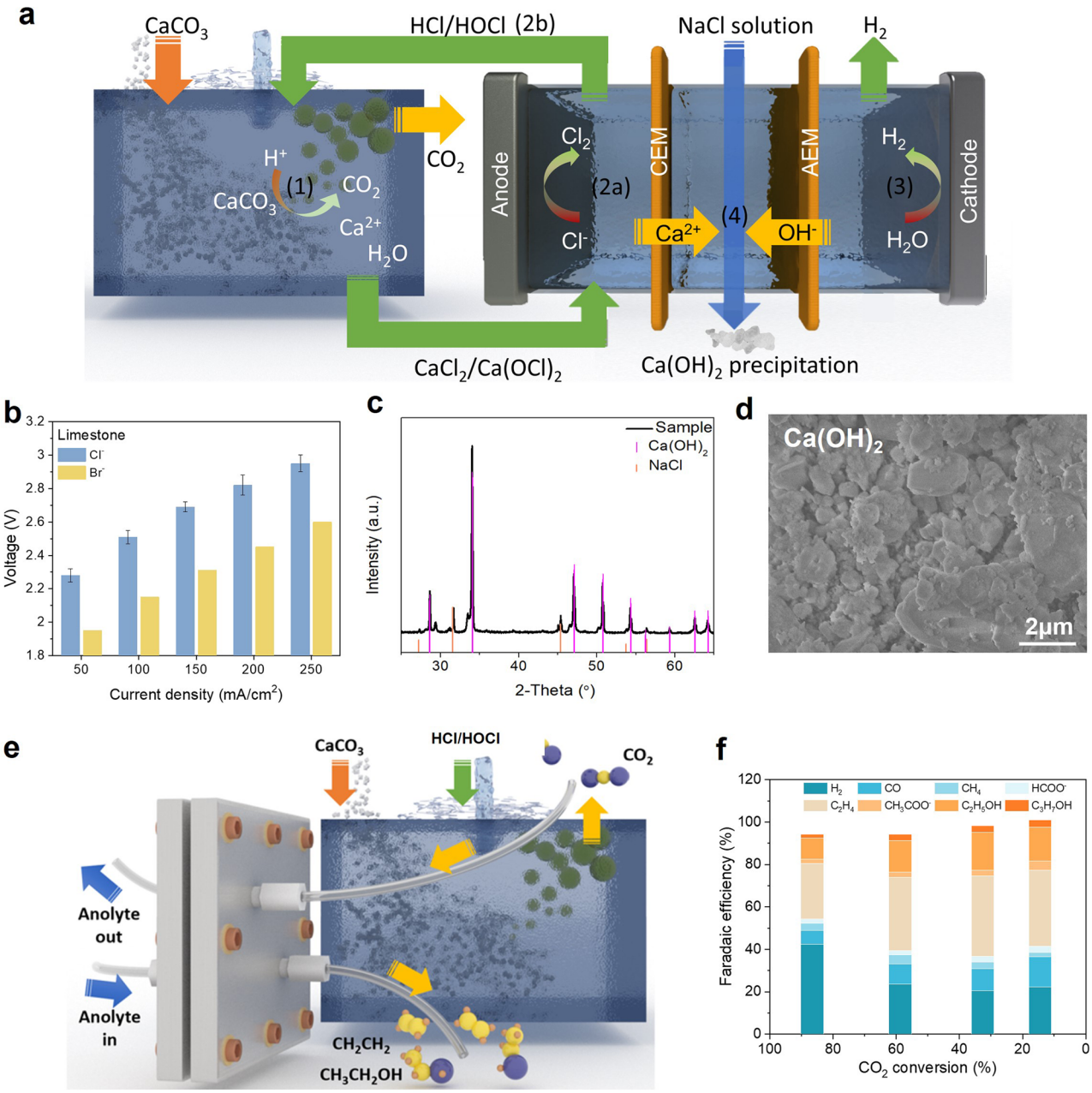

Figure 2. $Ca(OH)_2$ production in the electrochemical calcium extraction process. (a) Schematic of the ECE process to electrosynthesize $Ca(OH)_2$. (b) Voltage of the electrochemical unit at different current densities using limestone as the feedstock. (c) XRD pattern and (d) surface morphology of the electrosynthesized $Ca(OH)_2$ precipitate. (e) Schematic of the CO_2 removal unit paired with the CO_2 electrolyzer. (f) Faradaic efficiencies vs CO_2 conversion for the CO_2 electrolyzer.

halides, iodide offers the lowest thermodynamic potential but oxidizes to form a dense solid iodine layer on the electrode surface, which imposes a large charge-transfer resistance.[32] Bromine is a liquid at ambient temperature and pressure and does not result in layer formation. Therefore, we further adapted bromide as the anion and achieved a voltage of 2.4 V at 200 mA/cm^2, ~0.4 V lower than in the chloride case at the same current density (Figure 2b).

We collected and dried the white precipitate from the middle chamber (Figure S6b) and analyzed it using powder X-ray diffraction (XRD, Figure 2c). We confirmed the precipitate to be $Ca(OH)_2$ with a small amount of NaCl originating from the flowing electrolyte. Elemental analysis of the precipitate confirmed it to be predominantly calcium species. The chloride mass in the collected precipitate corresponds to ~0.2 wt% of the final cement weight—below the threshold limit (method details in Table S1).[33] We further demonstrated the use of a non-chloride salt as the flowing electrolyte, and the cell showed similar voltage to that of the NaCl case (Figure S10). Scanning electron microscopy (SEM, Figure 2d) showed that $Ca(OH)_2$ was made up of hexagonal nanocrystals. We further demonstrated that the collected high-purity CO_2 can be used to generate valuable precursors for industrial raw materials when coupled to a CO_2 electrolyzer with high conversion efficiency (Figure 2e,f).[34]

We adapted the ECE process to operate on carbon-free feedstocks and thereby eliminate both energy and feedstock emissions. To present a viable alternative, a carbon-free cement

https://doi.org/10.1021/acsenergylett.3c01668
ACS Energy Lett. 2023, 8, 4694−4701

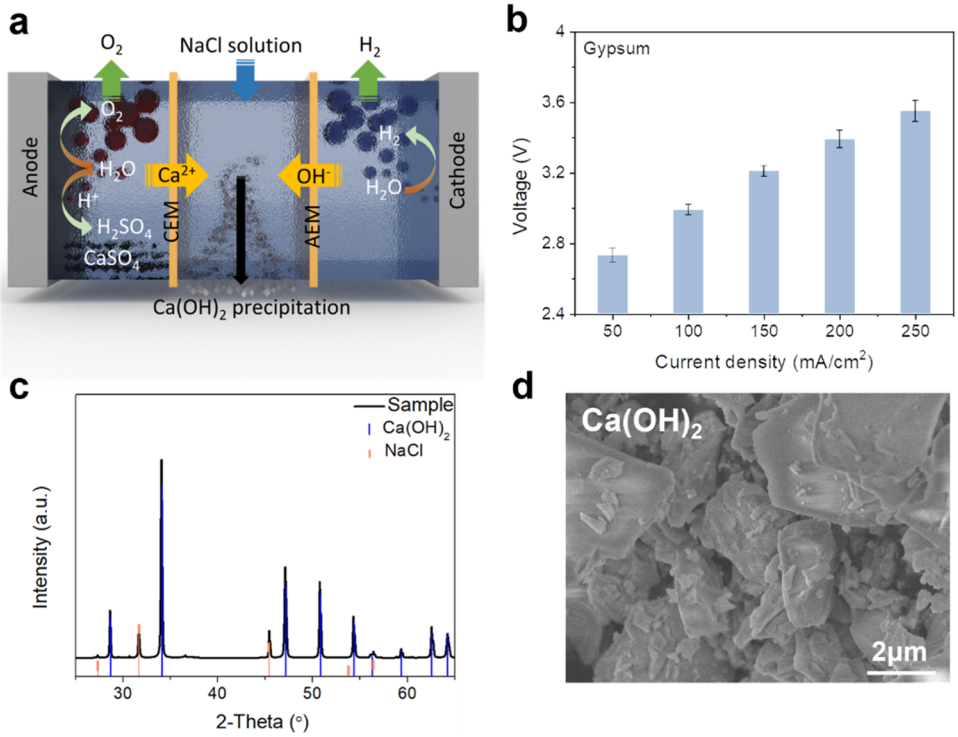

Figure 3. $Ca(OH)_2$ production in the electrochemical calcium extraction process by using gypsum as the feedstock. (a) Schematic of the ECE process to electrosynthesize $Ca(OH)_2$ from gypsum. (b) Voltage of the electrochemical unit at different current densities. (c) XRD pattern and (d) SEM surface morphology of the electrosynthesized $Ca(OH)_2$ precipitate.

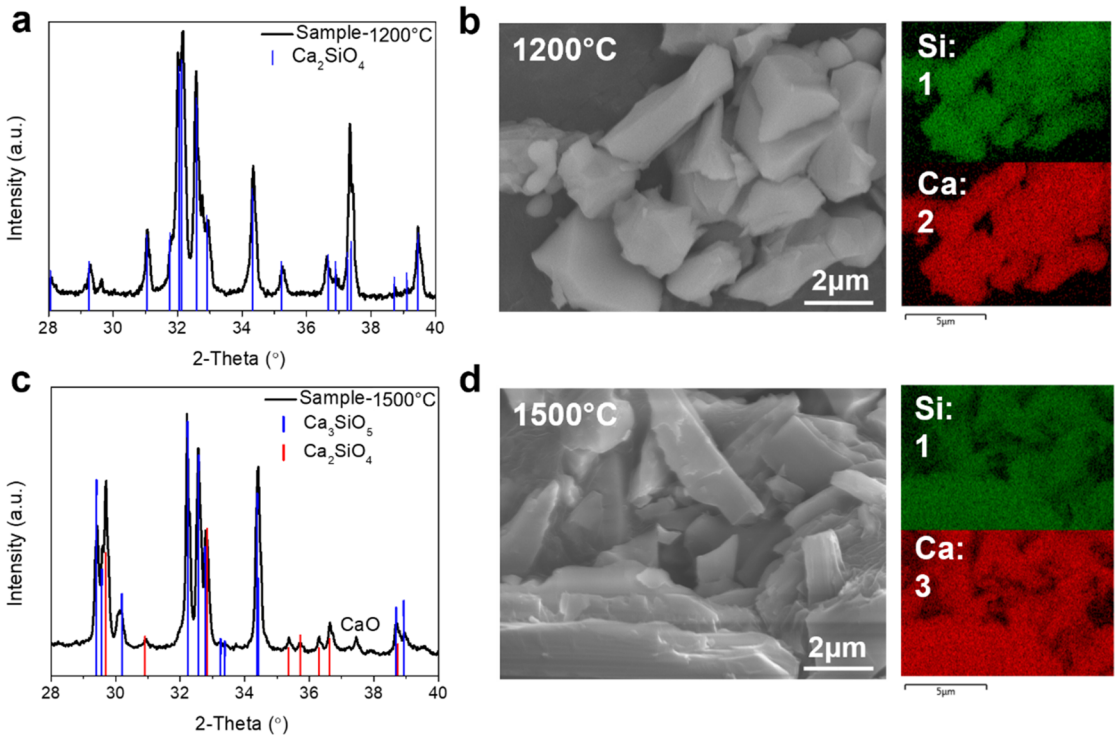

Figure 4. Synthesis of belite and alite using $Ca(OH)_2$ produced in the electrochemical calcium extraction process. XRD patterns of the produced belite and alite after sintering the $Ca(OH)_2$ and SiO_2 mixture (3:1 molar ratio) at (a) 1200 °C and (c) 1500 °C for 2 h in air. These patterns show single-phase belite and alite. Surface morphology of the produced belite and alite after sintering the $Ca(OH)_2$ and SiO_2 mixture (3:1 molar ratio) at (b) 1200 °C and (d) 1500 °C for 2 h in air.

feedstock is required that comes from naturally occurring salts with vast availability and low market price. Gypsum is a naturally occurring mineral with an annual production rate of 300 million metric tons[35] and is already used as a major cement additive (5% by mass of portland cement[18]). Today gypsum is not a viable alternative CaO source since it requires a higher temperature

https://doi.org/10.1021/acsenergylett.3c01668
ACS Energy Lett. 2023, 8, 4694−4701

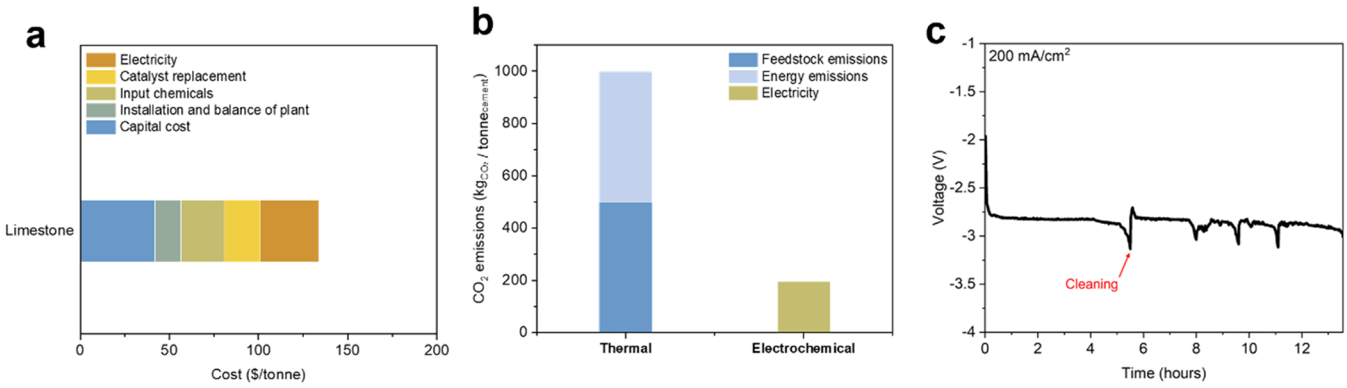

Figure 5. Technoeconomic analysis, life cycle analysis, and system stability of the electrochemical calcium extraction process. (a) TEA of the ECE process by using limestone as feedstock. TEA calculation details are provided in Note S1. (b) LCA of CO_2 emissions for the conventional thermal production process and the ECE process (with a cell voltage of 2.45 V and a current density of 200 mA/cm^2) to produce 1 tonne of cement. The carbon intensity of the electricity is 0.119 kg CO_2/kWh. (c) System voltage of $Ca(OH)_2$ synthesis by the ECE process over 13 h at 200 mA/cm^2.

(1300 °C) compared to limestone (900 °C) and emits a gaseous SO_2 stream when processed in conventional cement plants.[36] Through this electrochemical process, gypsum has the potential to address a portion of the current cement demand that is currently produced from carbon-intensive limestone.

We placed gypsum directly in the anode of our electrochemical unit to synthesize $Ca(OH)_2$ (Figure 3a). With the gypsum feedstock, acid neutralization was not required, so the oxygen evolution reaction was used as the anodic reaction. The electrochemical unit operating on gypsum required voltages slightly higher than that of the limestone feedstock, at the same current densities (Figure 3b). We associate the higher voltage with the lower solubility of gypsum (2.0−2.5 g/L at 25 °C; electrochemical impedance spectroscopy measurements and method details in Figure S9). Operating at 200 mA/cm^2, the cell voltage was 3.4 V. A white precipitate was once again collected in the middle chamber. XRD and SEM reveal $Ca(OH)_2$ having a similar surface morphology to when we began with limestone (Figure 3c,d). The current efficiency decreases over 2 h of electrolysis due to the low solubility of gypsum and accumulated H^+ in the electrolyte, with an average value of 83% (Figure S8). To ensure efficient operation, the acidic electrolyte must be replaced periodically, meaning a large volume of acidified water is generated. Approaches such as increasing the temperature and/or introducing additional soluble calcium salts into the electrolyte can increase gypsum solubility in the aqueous solution to lower the frequency of electrolyte replacement and should be investigated in the future.[37] However, with the current scenario, the large volume of acidified water should either be treated,[38,39] separated from water[40−43] (upon separation, the concentrated sulfuric acid can be sold as a byproduct at a market price of ∼$200/tonne[44]), or directly used in combination with other industrial processes. For example, diluted acid can be used for hydrolysis to produce bioethanol.[45]

We then sintered a mixture of $Ca(OH)_2$ and SiO_2 clinker in a 3:1 molar ratio to prepare portland cement. The H_2 co-generated from the electrochemical unit contained sufficient energy to fuel the subsequent sinter process (Note S2). We first sintered the mixed clinker at 1200 °C to confirm the formation of cement phases. After sintering the samples for 2 h at 1200 °C in air, XRD confirmed a transformation into the belite (Ca_2SiO_4) phase, a key phase (20−45% by mass of cement) in portland cement (Figure 4a). Energy-dispersive X-ray spectroscopy (EDS) mapping revealed that Ca and Si elements are—to within the 1 nm resolution available using this technique—distributed homogeneously within each phase. The elemental ratio from EDS showed Ca:Si is 2:1 (Figure S11a), consistent with belite (Figure 4a,b).

Further sintering to 1500 °C in air for 2 h resulted in belite combining with CaO to form alite (Ca_3SiO_5, Figure 4c),[46] the most abundant phase in portland cement. The alite particles produced from these precursors are 10−30 μm in size, in the range employed in portland cement (photographs in Figures S12 and S13). Ca_2SiO_4 and CaO were also detected in this sample, consistent with Ca_3SiO_5 thermal decomposition below 1250 °C.[47] EDS mapping and analysis of the elemental ratio showed Ca and Si distributed in the alite phase and a Ca:Si ratio of 3:1 (Figure 4d and Figure S11b) to within resolution limits.

We directly mixed limestone and SiO_2 to prepare the clinker under the same sintering condition (1500 °C) and found that the main phases were CaO and belite (Figure S14). The phase formation energy of alite was not reached since, relative to $Ca(OH)_2$, $CaCO_3$ requires more energy to dehydrate to CaO.[18] These results indicate that $Ca(OH)_2$ may be a more efficient feedstock for sintering than conventional $CaCO_3$.

We carried out a technoeconomic analysis (TEA, Note S1) to compare the cost of cement production using ECE to that of the conventional approach. We found the ECE process using limestone feedstock could produce cement at costs competitive with conventional, carbon-intensive production methods (Figure 5a). This cost comparison neglects the cost of carbon capture and sequestration in current cement production, which for amine scrubbing of conventional cement flue gas would add on the order of $90 per tonne cement.[14] We also include a TEA for the gypsum operation without any cost/value associated with downstream acid treatment and/or usage (Figure S15). The TEA shows that the ECE process using gypsum feedstock can produce cement at a cose competitive with the current market price, provided the acidic electrolyte brings value. We performed a life-cycle analysis (LCA) of the CO_2 emissions to make 1 tonne of cement, comparing the conventional thermal process with the ECE process (Figure 5b). The total emissions from the ECE process are dependent on the carbon intensity of the input electricity (Figure S16). Assuming a carbon intensity at a Canadian average (0.119 kg of CO_2/kWh), the LCA shows that cement production from the ECE process reduces CO_2

https://doi.org/10.1021/acsenergylett.3c01668
ACS Energy Lett. 2023, 8, 4694−4701

emissions by 80% compared to the thermal process. Further coupling the ECE process with an all-renewable electricity source offers a 93% reduction in CO_2 emissions compared to the thermal process (Figure S16).

We investigated the system stability at 200 mA/cm^2, during which we periodically provided a fresh calcium source for the $Ca(OH)_2$ synthesis. $Ca(OH)_2$ solids accumulate on membrane surfaces can lead to reduced ion transport and voltage degradation over time (Figure S17a). To address this issue, we performed periodic cleaning *in-operando* with a wiper insert in the electrolyzer (Figure S17b). With periodic *in-operando* cleaning, the voltage recovered to and was stable at ∼2.8 V for more than 13 h of continuous operation (Figure 5c). Post-reaction analysis of the electrodes using SEM revealed no structural changes of the IrO_2-Ti felt and Pt-carbon surface (Figure S18).

Here, we report an electrified cement production approach based on anion-mediated electrochemical calcium extraction. The *in situ*-generated acid is used to release CO_2 embodied within the feedstock, limestone at high purity, suitable for downstream sequestration and utilization. The $Ca(OH)_2$ and H_2 produced from the electrochemical unit can be used as feedstock and fuel, respectively, to produce portland cement. With this approach, we achieve a cell voltage of 2.8 V at 200 mA/cm^2, with a current efficiency of 93%. This corresponds to an energy cost of 6.7 GJ/tonne cement. We further demonstrate that the system can act on a carbon-free calcium feedstock, gypsum, to eliminate feedstock emissions. TEA and LCA indicate that the ECE process could produce portland cement at prices competitive with the current cement market price and with only 20% of emissions associated with the conventional thermal process.

■ ASSOCIATED CONTENT

Supporting Information

The Supporting Information is available free of charge at https://pubs.acs.org/doi/10.1021/acsenergylett.3c01668.

Methods; technoeconomic analysis; energy analysis; GC spectrum of the outlet gas from the CO_2 removal unit; exploded view of the electrochemical unit; SEM of the Pt/C; SEM of the IrO_2; validation of $Ca(OH)_2$ electrosynthesis; current efficiency calculation; EIS of the ECE process; elemental analysis of the precipitates; voltage using $NaNO_3$ as the flowing electrolyte; EDX of the cement; photographs of the prepared alite; characterizations of the prepared alite; XRD comparison of the cement; TEA of the ECE process by using gypsum as feedstock; life cycle analysis; device for the stability test; post-stability SEM images (PDF)

■ AUTHOR INFORMATION

Corresponding Authors

Edward H. Sargent − *Department of Electrical and Computer Engineering, University of Toronto, Toronto, Ontario M5S 3G4, Canada;* orcid.org/0000-0003-0396-6495; Email: ted.sargent@utoronto.ca

David Sinton − *Department of Mechanical and Industrial Engineering, University of Toronto, Toronto, Ontario M5S 3G8, Canada;* orcid.org/0000-0003-2714-6408; Email: sinton@mie.utoronto.ca

Authors

Rui Kai Miao − *Department of Mechanical and Industrial Engineering, University of Toronto, Toronto, Ontario M5S 3G8, Canada*

Ning Wang − *Department of Electrical and Computer Engineering, University of Toronto, Toronto, Ontario M5S 3G4, Canada;* orcid.org/0000-0002-2589-6881

Sung-Fu Hung − *Department of Applied Chemistry, National Yang Ming Chiao Tung University, Hsinchu 300, Taiwan, R.O.C.;* orcid.org/0000-0002-7423-2723

Wen-Yang Huang − *Department of Applied Chemistry, National Yang Ming Chiao Tung University, Hsinchu 300, Taiwan, R.O.C.*

Jinqiang Zhang − *Department of Mechanical and Industrial Engineering, University of Toronto, Toronto, Ontario M5S 3G8, Canada; Department of Electrical and Computer Engineering, University of Toronto, Toronto, Ontario M5S 3G4, Canada;* orcid.org/0000-0001-5476-0134

Yong Zhao − *Department of Mechanical and Industrial Engineering, University of Toronto, Toronto, Ontario M5S 3G8, Canada*

Pengfei Ou − *Department of Electrical and Computer Engineering, University of Toronto, Toronto, Ontario M5S 3G4, Canada;* orcid.org/0000-0002-3630-0385

Sasa Wang − *Department of Electrical and Computer Engineering, University of Toronto, Toronto, Ontario M5S 3G4, Canada*

Jonathan P. Edwards − *Department of Mechanical and Industrial Engineering, University of Toronto, Toronto, Ontario M5S 3G8, Canada;* orcid.org/0000-0003-4000-5802

Cong Tian − *Department of Electrical and Computer Engineering, University of Toronto, Toronto, Ontario M5S 3G4, Canada*

Jingrui Han − *School of Materials Science and Engineering and Key Laboratory of Efficient Utilization of Low and Medium Grade Energy, Ministry of Education, Tianjin University, Tianjin 300350, P. R. China*

Yi Xu − *Department of Mechanical and Industrial Engineering, University of Toronto, Toronto, Ontario M5S 3G8, Canada;* orcid.org/0000-0002-8108-0975

Mengyang Fan − *Department of Mechanical and Industrial Engineering, University of Toronto, Toronto, Ontario M5S 3G8, Canada*

Jianan Erick Huang − *Department of Electrical and Computer Engineering, University of Toronto, Toronto, Ontario M5S 3G4, Canada*

Yurou Celine Xiao − *Department of Mechanical and Industrial Engineering, University of Toronto, Toronto, Ontario M5S 3G8, Canada*

Alexander H. Ip − *Department of Electrical and Computer Engineering, University of Toronto, Toronto, Ontario M5S 3G4, Canada;* orcid.org/0000-0002-4604-4792

Hongyan Liang − *School of Materials Science and Engineering and Key Laboratory of Efficient Utilization of Low and Medium Grade Energy, Ministry of Education, Tianjin University, Tianjin 300350, P. R. China;* orcid.org/0000-0001-6623-6946

Complete contact information is available at: https://pubs.acs.org/10.1021/acsenergylett.3c01668

https://doi.org/10.1021/acsenergylett.3c01668
ACS Energy Lett. 2023, 8, 4694−4701

Author Contributions

[#]R.K.M. and N.W. contributed equally. E.H.S. and D.S. supervised the project. R.K.M. and N.W. conceived the idea and carried out the experiments. R.K.M., N.W., D.S., and E.H.S. co-wrote the paper. R.K.M. did the TEA calculation. S.-F.H., W.-Y.H., S.S.W. and Y.Z. conducted the oven, XRD and SEM measurements. J.Q.Z., Y.X., J.H., P.F.O., C.T., J.E.H., A.I. and H.Y.L. assisted in data analysis, manuscript writing and polishing. All authors discussed the results and assisted during manuscript preparation.

Notes

The authors declare no competing financial interest.

■ ACKNOWLEDGMENTS

The authors acknowledge support and infrastructure from the Natural Sciences and Engineering Research Council (NSERC) and the Government of Ontario through the Ontario Research Fund. R.K.M. thanks NSERC, Hatch, and the Government of Ontario for their support through graduate scholarships.

■ REFERENCES

(1) Fennell, P. S.; Davis, S. J.; Mohammed, A. Decarbonizing Cement Production. *Joule* **2021**, *5* (6), 1305−1311.

(2) Amato, I. Green Cement: Concrete Solutions. *Nature* **2013**, *494* (7437), 300−301.

(3) Habert, G.; Miller, S. A.; John, V. M.; Provis, J. L.; Favier, A.; Horvath, A.; Scrivener, K. L. Environmental Impacts and Decarbonization Strategies in the Cement and Concrete Industries. *Nat. Rev. Earth Environ.* **2020**, *1* (11), 559−573.

(4) USGS. *Cement Statistics and Information*, 2020. https://www.usgs.gov/centers/national-minerals-information-center/cement-statistics-and-information (accessed 2022-01-02).

(5) IEA. *Technology Roadmap - Low-Carbon Transition in the Cement Industry*, April 2018. https://www.iea.org/reports/technology-roadmap-low-carbon-transition-in-the-cement-industry

(6) Monteiro, P. J. M.; Miller, S. A.; Horvath, A. Towards Sustainable Concrete. *Nat. Mater.* **2017**, *16* (7), 698−699.

(7) Miller, S. A.; Moore, F. C. Climate and Health Damages from Global Concrete Production. *Nat. Clim. Chang.* **2020**, *10* (5), 439−443.

(8) Concrete Needs to Lose Its Colossal Carbon Footprint. *Nature* **2021**, *597* (7878), 593−594. .

(9) Ali, M. B.; Saidur, R.; Hossain, M. S. A Review on Emission Analysis in Cement Industries. *Renew. Sustain. Energy Rev.* **2011**, *15* (5), 2252−2261.

(10) Maddalena, R.; Roberts, J. J.; Hamilton, A. Can Portland Cement Be Replaced by Low-Carbon Alternative Materials? A Study on the Thermal Properties and Carbon Emissions of Innovative Cements. *J. Clean. Prod.* **2018**, *186*, 933−942.

(11) Daehn, K.; Basuhi, R.; Gregory, J.; Berlinger, M.; Somjit, V.; Olivetti, E. A. Innovations to Decarbonize Materials Industries. *Nat. Rev. Mater.* **2022**, *7*, 275−294.

(12) Sutter, D.; Werner, M.; Zappone, A.; Mazzotti, M. Developing CCS into a Realistic Option in a Country's Energy Strategy. *Energy Procedia* **2013**, *37*, 6562−6570.

(13) De Lena, E.; Spinelli, M.; Gatti, M.; Scaccabarozzi, R.; Campanari, S.; Consonni, S.; Cinti, G.; Romano, M. C. Techno-Economic Analysis of Calcium Looping Processes for Low CO_2 Emission Cement Plants. *Int. J. Greenh. Gas Control* **2019**, *82*, 244−260.

(14) Gardarsdottir, S. O.; De Lena, E.; Romano, M.; Roussanaly, S.; Voldsund, M.; Pérez-Calvo, J. F.; Berstad, D.; Fu, C.; Anantharaman, R.; Sutter, D.; Gazzani, M.; Mazzotti, M.; Cinti, G. Comparison of Technologies for CO_2 Capture from Cement Production—Part 2: Cost Analysis. *Energies* **2019**, *12* (3), 542.

(15) *Cementing the European Green Deal. Reaching Climate Neutrality along the Cement and Concrete Value Chain by 2050*; The European Cement Association, Brussels, 2020. https://cembureau.eu/library/reports/2050-carbon-neutrality-roadmawp/

(16) Li, S.; Jiang, N.; Zhou, K.; Jiao, X. Rotary Kiln for Producing Lime through Calcination by Using Electric Heating Device. CN201210117384.6A, April 20, 2012.

(17) Habert, G.; Billard, C.; Rossi, P.; Chen, C.; Roussel, N. Cement Production Technology Improvement Compared to Factor 4 Objectives. *Cem. Concr. Res.* **2010**, *40* (5), 820−826.

(18) Imbabi, M. S.; Carrigan, C.; McKenna, S. Trends and Developments in Green Cement and Concrete Technology. *Int. J. Sustain. Built Environ.* **2012**, *1* (2), 194−216.

(19) Snellings, R.; Mertens, G.; Elsen, J. Supplementary Cementitious Materials. *Rev. Mineral. Geochem.* **2012**, *74* (1), 211−278.

(20) Bentz, D. P.; Hansen, A. S.; Guynn, J. M. Optimization of Cement and Fly Ash Particle Sizes to Produce Sustainable Concretes. *Cem. Concr. Compos.* **2011**, *33* (8), 824−831.

(21) Gartner, E. M.; MacPhee, D. E. A Physico-Chemical Basis for Novel Cementitious Binders. *Cem. Concr. Res.* **2011**, *41* (7), 736−749.

(22) Schneider, M.; Romer, M.; Tschudin, M.; Bolio, H. Sustainable Cement Production—Present and Future. *Cem. Concr. Res.* **2011**, *41* (7), 642−650.

(23) Gartner, E.; Sui, T. Alternative Cement Clinkers. *Cem. Concr. Res.* **2018**, *114*, 27−39.

(24) Ellis, L. D.; Badel, A. F.; Chiang, M. L.; Park, R. J. Y.; Chiang, Y. M. Toward Electrochemical Synthesis of Cement—An Electrolyzer-Based Process for Decarbonating CaCO3 While Producing Useful Gas Streams. *Proc. Natl. Acad. Sci. U. S. A.* **2020**, *117* (23), 12584−12591.

(25) Zhang, Z.; Mowbray, B. A. W.; Parkyn, C. T. E.; Waizenegger, C.; Williams, A. S. R.; Lees, E. W.; Ren, S.; Kim, Y.; Jansonius, R. P.; Berlinguette, C. P. Cement Clinker Precursor Production in an Electrolyser. *Energy Environ. Sci.* **2022**, *15* (12), 5129−5136.

(26) Mowbray, B. A. W.; Zhang, Z. B.; Parkyn, C. T. E.; Berlinguette, C. P. Electrochemical Cement Clinker Precursor Production at Low Voltages. *ACS Energy Lett.* **2023**, *8*, 1772−1778.

(27) Boot-Handford, M. E.; Abanades, J. C.; Anthony, E. J.; Blunt, M. J.; Brandani, S.; Mac Dowell, N.; Fernández, J. R.; Ferrari, M. C.; Gross, R.; Hallett, J. P.; Haszeldine, R. S.; Heptonstall, P.; Lyngfelt, A.; Makuch, Z.; Mangano, E.; Porter, R. T. J.; Pourkashanian, M.; Rochelle, G. T.; Shah, N.; Yao, J. G.; Fennell, P. S. Carbon Capture and Storage Update. *Energy Environ. Sci.* **2014**, *7* (1), 130−189.

(28) Sullivan, I.; Goryachev, A.; Digdaya, I. A.; Li, X.; Atwater, H. A.; Vermaas, D. A.; Xiang, C. Coupling Electrochemical CO_2 Conversion with CO_2 Capture. *Nat. Catal.* **2021**, *4* (11), 952−958.

(29) Leow, W. R.; Lum, Y.; Ozden, A.; Wang, Y.; Nam, D. H.; Chen, B.; Wicks, J.; Zhuang, T. T.; Li, F.; Sinton, D.; Sargent, E. H. Chloride-Mediated Selective Electrosynthesis of Ethylene and Propylene Oxides at High Current Density. *Science* **2020**, *368* (6496), 1228−1233.

(30) Subbaraman, R.; Tripkovic, D.; Strmcnik, D.; Chang, K. C.; Uchimura, M.; Paulikas, A. P.; Stamenkovic, V.; Markovic, N. M. Enhancing Hydrogen Evolution Activity in Water Splitting by Tailoring Li+-Ni(OH)2-Pt Interfaces. *Science* **2011**, *334* (6060), 1256−1260.

(31) Rosestolato, D.; Fregoni, J.; Ferro, S.; De Battisti, A. Influence of the Nature of the Electrode Material and Process Variables on the Kinetics of the Chlorine Evolution Reaction. The Case of IrO2-Based Electrocatalysts. *Electrochim. Acta* **2014**, *139*, 180−189.

(32) Jang, W. J.; Cha, J. S.; Kim, H.; Yang, J. H. Effect of an Iodine Film on Charge-Transfer Resistance during the Electro-Oxidation of Iodide in Redox Flow Batteries. *ACS Appl. Mater. Interfaces* **2021**, *13* (5), 6385−6393.

(33) Falaciński, P.; Machowska, A.; Szarek, Ł. The Impact of Chloride and Sulphate Aggressiveness on the Microstructure and Phase Composition of Fly Ash-Slag Mortar. *Materials* **2021**, *14* (16), 4430.

(34) O'Brien, C. P.; Miao, R. K.; Liu, S.; Xu, Y.; Lee, G.; Robb, A.; Huang, J. E.; Xie, K.; Bertens, K.; Gabardo, C. M.; Edwards, J. P.; Dinh, C. T.; Sargent, E. H.; Sinton, D. Single Pass CO_2 Conversion Exceeding 85% in the Electrosynthesis of Multicarbon Products via Local CO_2 Regeneration. *ACS Energy Lett.* **2021**, *6*, 2952−2959.

(35) National Minerals Information Center, USGS. *Mineral Commodities Summary*, Feb 7, 2020. https://www.usgs.gov/media/images/mineral-commodities-february-2020

(36) Swift, W. M.; Panek, A. F.; Smith, G. W.; Vogel, G. J.; Jonke, A. A. Decomposition of Calcium Sulfate: A Review of the Literature. OSTI.GOV Technical Report, 1976. DOI: 10.2172/7224692.
(37) Klimchouk, A. The Dissolution and Conversion of Gypsum and Anhydrite. *Int. J. Speleol.* **1996**, *25* (3), 21−36.
(38) Jarnerud, T.; Karasev, A. V.; Jönsson, P. G. Neutralization of Acidic Wastewater from a Steel Plant by Using CaO-Containing Waste Materials from Pulp and Paper Industries. *Materials (Basel)* **2021**, *14* (10), 2653.
(39) Leiva, E.; Leiva-Aravena, E.; Vargas, I. Acid Water Neutralization Using Microbial Fuel Cells: An Alternative for Acid Mine Drainage Treatment. *Water* **2016**, *8* (11), 536.
(40) Cao, Y.; Luo, J.; Chen, C.; Wan, Y. Highly Permeable Acid-Resistant Nanofiltration Membrane Based on a Novel Sulfonamide Aqueous Monomer for Efficient Acidic Wastewater Treatment. *Chem. Eng. J.* **2021**, *425*, No. 131791.
(41) Qifeng, W.; Xiulian, R.; jingjing, G.; Yongxing, C. Recovery and Separation of Sulfuric Acid and Iron from Dilute Acidic Sulfate Effluent and Waste Sulfuric Acid by Solvent Extraction and Stripping. *J. Hazard. Mater.* **2016**, *304*, 1−9.
(42) Wei, C.; Li, X.; Deng, Z.; Fan, G.; Li, M.; Li, C. Recovery of H2SO4 from an Acid Leach Solution by Diffusion Dialysis. *J. Hazard. Mater.* **2010**, *176* (1−3), 226−230.
(43) Kesieme, U. K.; Milne, N.; Cheng, C. Y.; Aral, H.; Duke, M. Recovery of Water and Acid from Leach Solutions Using Direct Contact Membrane Distillation. *Water Sci. Technol.* **2014**, *69* (4), 868−875.
(44) Procurement Resource. *Sulfuric Acid Prices: Latest Price, Pricing, News, Market Analysis*. https://www.procurementresource.com/resource-center/sulfuric-acid-price-trends (accessed 2023-10-03).
(45) Quintero, J. A.; Rincón, L. E.; Cardona, C. A. Production of Bioethanol from Agroindustrial Residues as Feedstocks. *Biofuels Altern. Feed. Convers. Process.* **2011**, 251−285.
(46) Cement Kilns. *Clinker Thermochemistry*. https://www.cementkilns.co.uk/ckr_therm.html (accessed 2023-05-12).
(47) Mohan, K.; Glasser, F. P. The Thermal Decomposition of Ca_3SiO_5 at Temperatures below 1250°C I. Pure C_3S and the Influence of Excess CaO or Ca_2SiO_4. *Cem. Concr. Res.* **1977**, *7* (1), 1−7.

https://doi.org/10.1021/acsenergylett.3c01668
ACS Energy Lett. 2023, 8, 4694−4701